Evaluation of Rock Debris Based on Particle Shapes and Sizes

Mária Bali Hudáková[1*)], Víťazoslav Krúpa[2)], Alexander Kiovský[3)], Pavol Vavrek[4)], Edita Lazarová[5)], Lucia Ivaničová[6)]

[1*)] Institute of Geotechnics of the Slovak Academy of Sciences, Watsonova 45, SK-04001 Košice, Slovakia; E-mail: krulakova@saske.sk; https://orcid.org/0000-0002-3897-4762
[2)] Institute of Geotechnics of the Slovak Academy of Sciences, Watsonova 45, SK-04001 Košice, Slovakia; E-mail; krupa@saske.sk; https://orcid.org/0009-0004-5030-0914
[3)] Institute of Geotechnics of the Slovak Academy of Sciences, Watsonova 45, SK-04001 Košice, Slovakia; E-mail; kiovsky@saske.sk; https://orcid.org/0009-0002-7278-0360
[4)] Institute of Geotechnics of the Slovak Academy of Sciences, Watsonova 45, SK-04001 Košice, Slovakia; E-mail; vavrek@saske.sk; https://orcid.org/0000-0002-1125-1361
[5)] Institute of Geotechnics of the Slovak Academy of Sciences, Watsonova 45, SK-04001 Košice, Slovakia; E-mail; lazarova@saske.sk; https://orcid.org/0000-0003-4682-6433
[6)] Institute of Geotechnics of the Slovak Academy of Sciences, Watsonova 45, SK-04001 Košice, Slovakia; E-mail; ivanic@saske.sk; https://orcid.org/0000-0003-3844-9703

https://doi.org/10.29227/IM-2026-02-02-023

Submission date: *2026-09-04* | Review date: *2026-24-04*

Abstract

This study focuses on characterizing the shape of drill cuttings produced during drilling in limestone, andesite, and granodiorite. These rock debris particles were collected in containers during drilling as a result of rock disintegration. The drill cuttings were analyzed using wet-sieve analysis with six sieves of different mesh sizes. The rock debris was divided into seven classes. When evaluating particle shape, we focus on the second class, which has the largest particles, ranging from 400 µm to 1000 µm, but accounts for the lowest percentage of the total weight of drilling debris. Particle size distribution was measured using the Camsizer X2 particle size and shape analyzer (Retsch, Germany) with dual camera technology and an X-dry sample feeder. From data obtained from the particle analyzer, we evaluated particle shape using diagrams by Sneed & Folk, which categorize drill cuttings into seven descriptive classes. Through this analysis, we aimed to gather information about the interaction between rocks and surface-set diamond core drill bits. The aim was to monitor changes in the shape and size of particles from the analyzed larger rock fragments after drilling rock samples. Changes in particle size relative to their shape were assessed using a calculated shape coefficient. The coefficient is represented by a single number for each rock specimen. Using the coefficient, we can identify changes in the constant drilling regimes, including the drilled length and the type of drilling tool used. Such an assessment of particle shape would help provide a more detailed evaluation of the selection of drilling tools and their wear.

Keywords: *rock debris, particle size distribution, shape coefficient, rock disintegration.*

1. Introduction

Mechanical rotational rock disintegration methods are based on the contact and force action of disintegrating elements (indenters) on the rock. At the contact point, frictional forces and movement are converted into energy, which causes the rock's surface layer to break. The rock is macroscopically disturbed up to the point of disconnection, while the indenter is microscopically damaged. Microscopical damage to the indenter is referred to as wear, while macroscopical damage is called damage. This process is influenced by various factors, including the structural diversity of rocks, their anisotropy, the formation of microcracks during the removal of rock samples from the natural stress field, the degree of weathering, the presence of water in the pores, and similar factors. The mechanical properties of the test rocks are significantly influenced by their texture [1]. The rock's strength plays a key role in disconnection and is fundamentally affected by the quantity, size, and orientation of its defects. It is defined as the value of the contact shear stress at the point of disconnection. Contact stress (the intensity of internal forces) is derived from the intensity of external force loading, calculated as the ratio of the external force to the contact area. It is assumed that the intensity of external and internal forces is the same. The rock's strength is also significantly influenced by the degree of weathering.

Due to stress and deformation at the rock-tool interface, brittle failure occurs in a small volume of material beneath the rock surface. This principle forms the basis of all mechanical rock disintegration techniques: applying a thrust force to the working tool to penetrate the rock and break it into debris. The product of rock disintegration can be characterized by the size of the resulting rock debris. Achieving a fine-grained breaking product requires higher energy expenditure. This axiom is explained by several energy and technological theories of material breaking. Therefore, the amount of energy consumed for breaking is not a property of the material being broken but is a function of the process, which is influenced by the properties of the material being broken and the properties of the contact surfaces of the indenter [2].

Methods of image analysis and visual comparison are used to measure the shape properties of granular materials [3]. Quantitative shape measurements can be performed on two-dimensional images or projections of particles, or on the three-dimensional shape of individual particles. On the other hand, 2D imaging cannot illustrate particle shapes, as particles are often positioned at larger sizes, and smaller particles may be ignored; particle projection can also change with particle rotation or the viewing angle [4]. Standardized numerical shape indices have been developed to facilitate particle shape analysis through

mathematical or graphical methods. Analytical equations based on particle size distribution (PSD) are derived from indirect methods [5], [6]. Several researchers have attempted to define the overall shape of particles using the longest, median, and shortest orthogonal axes (L, I, S), which can yield the same results for different shapes [1], [7]. These relationships are used to describe rock debris as rounded (compact or equant), disc-shaped, blade-shaped, or elongated/rod-like. The description of two-dimensional particle shape is generally used to determine wear and weathering during transport, whereas the three-dimensional shape is more closely related to the particles' lithology.

The two-dimensional shape description in this study was based on particle size distributions from image analysis and triangular diagrams [8], [9]. Triangular diagrams are a standard method for presenting data on primary particle shape because they preserve symmetries across the continuum of shapes without deformation.

The main objectives of this study can be summarized as follows: (a) to describe the interaction between rock and tool using two types of drilling bits and three rock samples with an experimental drilling setup in laboratory conditions; (b) processing of rock debris using wet-sieve analysis after drilling rock samples; (c) to analyze in detail the shape and size of rock debris by measuring the geometric features of rock particles, which will help us calculate the shape coefficient; (d) to present various mechanical properties of rocks and show how they relate to the shape coefficient.

2. Research methodology

Rock debris samples for assessing particle shape and size were collected after drilling limestone, granodiorite, and andesite. Rock samples were drilled using an experimental drilling rig in laboratory conditions. The properties of the rock samples used are listed in Table 1.

Tab. 1. Selected mechanical properties of the tested rock samples.

Properties of rock samples	Limestone	Granodiorite	Andesite
Uniaxial compressive strength (MPa)	85.1	85.8	208
Tangent Young´s Modulus (GPa)	82.3	65.8	101.251
Pin abrasivity index ($mg.m^{-1}$)	0.0186	1.4092	0.7913
Brinell hardness ($kg.mm^{-2}$)	466.4	831.1	5,921
Indentation strength (MPa)	2,366	2,904	5,211

According to Table 1, andesite has the highest uniaxial compressive strength (UCS), indicating greater resistance to local and volumetric stresses. Granodiorite is the most abrasive, which can accelerate the wear of diamond grains on drill bit working surfaces.

Through these experiments, we aimed to gather information about the interaction between rocks and surface-set diamond core drill bits. The individual boreholes were divided into the following sections:

- Drilling limestone and granodiorite samples with two surface-set 3-channel drill bits with different diamond sizes: 16/25 (stones per carat) and 25/40 (stones per carat).
- Drilling limestone and andesite samples with two surface-set 3-channel drill bits of the same diamond size:16/25(stones per carat).

Drilling limestone (L1-L9) samples focused on rock debris evaluation after drilling a constant length of 1 meter. After approximately 6.75 meters, drilling into granodiorite was initiated to accelerate the deterioration of the surface-set diamond drill bits. Drilling into granodiorite was conducted on 3 samples (G1-G3). Table 2 describes the applied drilling modes (thrust force F (kN) and constant rotation speed of the drill bit at 1,000 rpm) used for limestone and granodiorite with both drill bit types.

Drilling limestone (L11- L16) and andesite (A1 -A6) samples focused on various regime parameters, see Tab. 3. Table 3 shows the drilling modes, including thrust force F (kN) and drill bit rotation speed n (rpm), used for limestone and andesite with both types of drill bits.

The aim was to monitor changes in the shape and size of particles from the analyzed larger rock fragments after drilling rock samples. During horizontal rotary drilling into limestone, andesite, and granodiorite, flushing water and disintegrated rocks were collected in collection vessels for rock debris analysis. The rock debris was analyzed using wet-sieve analysis, with water used as the flushing fluid during drilling at a volumetric rate of 10^{-3} m^3/s.

Samples of rock debris were classified into seven categories based on the sieves used, with fractions: W1: > 1,000 µm; W2: 1,000 µm – 400 µm; W3: 400 µm – 200 µm; W4: 200 µm – 160 µm; W5: 160 µm – 80 µm; W6: 80 µm – 40 µm; W7: < 40 µm.

In Tables 2 and 3, the total mass of drilling debris, m (g), and the percentage representation of class W2 (%) are provided. When evaluating particle shape, we focus on the second class, W2, which has the largest particles, ranging from 400 µm to 1000 µm, but accounts for the lowest percentage of the total weight of drilling debris.

2.1 Measurement of particle shape and size

The setup of the experimental processing of the fraction W2 drill cuttings involved four parts: particle size analysis using CamsizerX2 software, entering data into the Tri-Plot worksheet in Excel from CamsizerX2 software to plot the Sneed and Folks class areas, calculating the percentage distribution of individual particle shapes from the classified Sneed and Folks diagrams, and calculating the shape coefficient.

Particle size distribution was measured using the Camsizer X2 particle size and shape analyzer (Retsch, Germany) with dual camera technology and an X-dry sample feeder. The measuring range was set to 0.4-1 mm for all the tested samples of rock debris.

The Camsizer X2 program calculated the average particle size in each size class as a reference value for the shortest (xc_min3), longest (xFe_max3), and mean (x_mean3) particle dimensions in millimeters. Based on the volumetric analysis of particle sizes, divided into fractional intervals that are consistent across all samples of rock debris W2, the particle shape was subsequently determined using Sneed & Folk diagrams in the Tri-Plot worksheet in Excel [9].

2.2 Sneed and Folk Diagram

The diagram shows the seven particle shapes captured by the Camsizer X2, as illustrated in Fig. 1. The labels are C for Compatibility, CB for Compact Blades, CE for Compact Elongated, P for Plates, B for Blades, and E for Elongated.

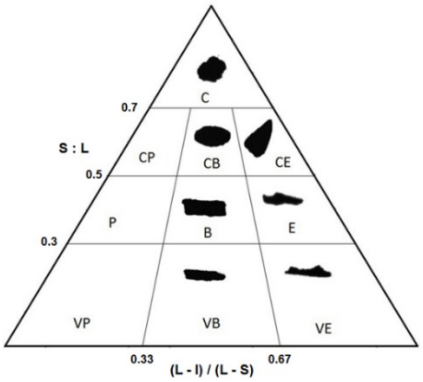

Fig. 1. The 10 descriptive classes for schematic particle shape classification diagram defined by Sneed and Folk, [8]: C-compact, P-platy, B-bladed, E-elongate, V-very.

Particles can be classified as compact (C), platy (P), bladed (B), or elongated (E) based on the Sneed and Folks diagram. Since it utilizes three orthogonal particle axes (S- short, L-long, I-intermediate), it is recommended as the most impartial method for presenting primary particle shape data. It employs a combination of the compactness ratio (L-I)/(L-S) and the form factor F, as shown in Fig. 1, to define any point within the triangle's boundaries. Particles with F<0.33 are classified as platy; those with 0.33<F<0.67 are long, thin-bladed; and particles with F>0.67 are elongated.

The degree of compactness, S-sphericity, is also used to categorize particle forms into orders, but in a different way. For example, when S is more than 0.7, a sphere-like arrangement is produced, and when S is between 0.5 and 0.70, the shape is somewhere between compact platy (CP) and bladed (CB) or elongated (CE). The particles are very platy (VP), bladed (VB), or elongated (VE) if S-sphericity is less than 0.3 or 0.5. If S is less than 0.3, they are classified as very platy (VP), [9], [10].

The calculated shape distributions of the particles of the analyzed class W2 are shown in Fig. 2 and Fig. 3. Where L1 - L9 are rock samples of drilled limestone, and G1 - G3 are drilled samples of granodiorite with two drill bits of different diamond sizes.

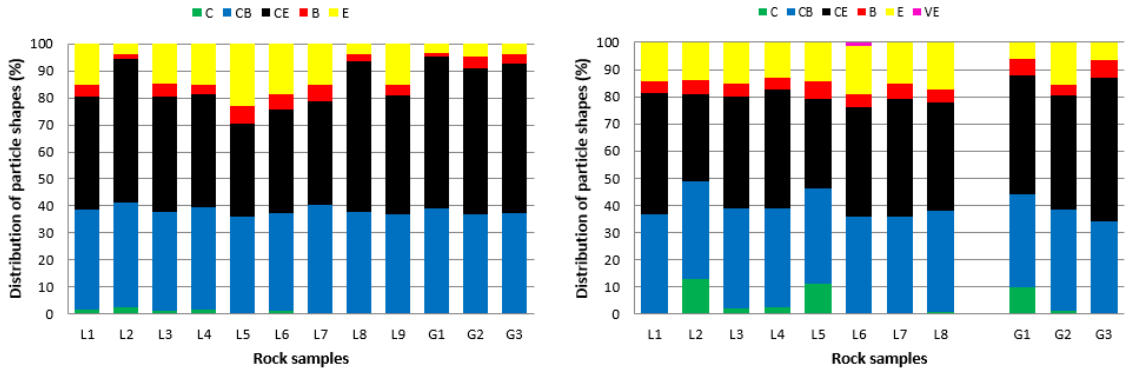

Fig. 2. Distribution of particle shapes of the analyzed class W2 with fractions (1mm – 0,4 mm) of drilling into limestone (L1-L9) and granodiorite (G1-G3) using drill bits: 16/25 (left) and 25/40 (right).

From these particle shape classifications, it is evident that when using the 25/40 drill bit, the shape of particles labeled as E-Elongated was present in the same percentage for all drilled limestone samples L1-L9, Fig. 2 (right).

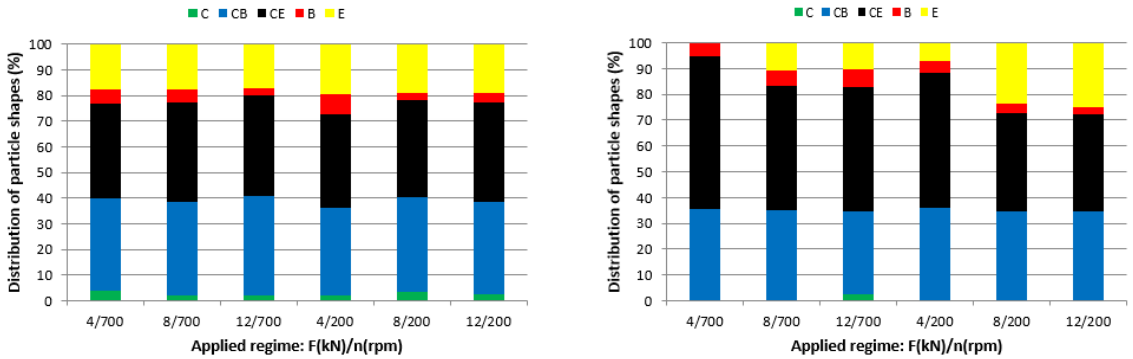

Fig. 3. Distribution of particle shapes of the analyzed class W2 with fractions (1mm – 0,4 mm) of drilling into limestone (left) and andesite (right) using drill bit: 16/25.

2.3 Calculating the shape coefficient

The shape coefficient FC was calculated from particle-size and shape analyses of the analyzed class W2 rock fragments, using Sneed & Folk diagrams in the Tri-Plot worksheet in Excel. Tables 2 and 3 detail the calculated particle shapes (C, CB, CE, B, E, VE) and their corresponding size distributions.

Tab. 2. The grain-size distribution is characterized by particle shape for two drill bits, 16/25 and 25/40.

Rock sample (drill bit)	C (mm)	CB (mm)	CE (mm)	B (mm)	E (mm)	VE (mm)	F (kN)	Total drilled length (m)	Drilled length (mm)	m (g)	W2 (%)
L_3(16/25)	1-1.04	0.52-1.04	0.4-1	0.4-0.48	0.4, 1.04		16	5.51	200	502.62	6.59
L_3(25/40)	0.92-1.04	0.52-1.04	0.4-0.96	0.4-0.48	0.4, 1-1.04		15.8	5.51	200	512.3	6.32
L_4(16/25)	1-1.04	0.52-1.04	0.4-1	0.4-0.48	0.4, 1.04		16.3	6.75	200	535.79	7.54
L_4(25/40)	0.8, 0.96-1.04	0.52-1.04	0.4-1	0.4-0.48	0.4, 1.04		15.6	6.75	200	560.63	6.97
G_1(16/25)	0.52	0.48-1.04	0.4–1.04	0.4-0.44	0.4		9	6.93	180	493.61	1.85
G_1(25/40)	0.6-0.72, 0.88-1	0.52-1.04	0.4–1.04	0.4-0.48	0.4		9	7.13	180	450.12	0.27
L_7(16/25)		0.52-1.04	0.4–1.04	0.4-0.48	0.4-0.44, 0.92-1.04		18	7.68	200	520.23	1.71
L_6(25/40)		0.56-1.04	0.4-1.04	0.44-0.52	0.4, 0.96-1.04	0.4, 1.04	17.3	7.33	200	502.91	1.88
G_2(16/25)	0.52	0.52-1.04	0.4-1.04	0.4-0.48	0.4		9.2	7.83	150	379.69	0.18
G_2(25/40)	1-1.04	0.52-1.04	0.4-1	0.4-0.44	0.4, 1.04		9.7	7.48	150	379.9	0.21
L_8(16/25)		0.52-1.04	0.4-1.04	0.4-0.48	0.4		17	8.03	200	482.96	0.9
L_7(25/40)		0.56-1.04	0.4-1.04	0.4-0.52	0.4, 1.04		17.3	7.68	200	459.17	0.27
G_3(16/25)		0.52-1.04	0.4-1.04	0.4-0.48	0.4		16	8.18	150	371.29	0.29
G_3(25/40)		0.52-1.04	0.4-1.04	0.4-0.48	0.4		13.9	7.83	150	371.61	0.1
L_9(16/25)		0.52-1.04	0.4–1.04	0.4-0.48	0.4		18	8.38	200	481.14	0.35
L_8(25/40)	1.04	0.52-1.04	0.4–1.04	0.4-0.48	0.4, 0.96-1.04		17	8.03	200	496.66	0.88

Tab. 3. The grain-size distribution, characterized by particle shape, for two drill bits, 16/25.

Rock sample	C (mm)	CB (mm)	CE (mm)	B (mm)	E (mm)	F (kN)	n (rpm)	Drilled length (mm)	m (g)	W2 (%)
L_{11}	0.96-1.04	0.56-1.04	0.4-1	0.4-0.52	0.4-0.44 1.04	4	700	60	168.74	7.8
L_{12}	1.04	0.56-1.04	0.44–1	0.4-0.52	0.4, 1.04	8	700	140	358.14	7.05
L_{13}	1.04	0.52-1.04	0.4-1	0.4-0.48	0.4, 1.04	12	700	140	398.9	10.19
A_1	1	0.48-1.04	0.4-1.04	0.4-0.44		4	700	60	134.29	0.36
A_2		0.48-0.96, 1.04	0.4–1.04	0.4-0.44	0.4, 0.48, 0.92-1	8	700	140	345.89	0.57
A_3	1	0.48-1	0.4-1.04	0.4-0.44	0.4, 0.92	12	700	140	321.63	0.39
L_{14}	0.88, 1-1.04	0.56-1.04	0.4-0.96	0.4-0.52	0.4-0.48, 0.92-1.04	4	200	60	195.55	8.07
L_{15}	0.92-1.04	0.52-1.04	0.4-1	0.44-0.48	0.4-0.56, 1.04	8	200	60	161.39	7.6
L_{16}	1.04	0.56-1.04	0.4-1	0.44-0.52	0.4, 1.04	12	200	100	235.48	8.36
A_4		0.48-0.96, 1.04	0.4-1.04	0.4-0.44	0.4	4	200	60	125.96	1.17
A_5		0.52-1.04	0.4-1.04	0.44-0.48	0.4-0.48, 0.92-1.04	8	200	60	121.23	1.42
A_6		0.48-1.04	0.4-1.04	0.44	0.4-0.48, 0.84-1.04	12	200	100	250.6	1.37

Based on this classification, calculations were subsequently made to determine the arithmetic mean size FF_1 (mm) of all particles N_1 and the arithmetic mean size FF_0 (mm) of all particles N_0.

N_1 (%) represents the sum of the percentage representation of particles with shapes E-Elongated, B-Blade, and VE-Very Elongated, where the aspect ratio of the grain is greater than 2.

N_0 (%) represents the sum of the percentage representation of particles with shapes C-Compact, CE-Compact Elongated, and CB-Compact Blades, where the aspect ratio of the grain is less than 2. The percentage representation of particles with concrete shapes is shown in Fig. 2 and Fig. 3. The geometric parameter used to evaluate particle shape was elongation, defined as the grain's aspect ratio. This is simply defined as the ratio of the grain's length to its width from two orthogonal particle axes (L-long, S-short).

The shape coefficient FC was calculated according to equation (1), whose values are shown in Tables 4 and 5.

$$FC = \frac{\left(\frac{N_0}{N_0+N_1}\cdot\frac{1}{FF_0}\right)}{\left(\frac{N_1}{N_0+N_1}\cdot\frac{1}{FF_1}\right)} = \frac{N_0 FF_1}{N_1 FF_0} \quad (1)$$

From tables 4 and 5, it can be seen that the decrease in elongated particles N_1 increased the proportion of compact N_0, which caused an increase in the shape factor FC. Furthermore, higher specific energy values indicate an increase in the shape coefficient FC, which was derived from a larger fraction W2 of rock debris.

Tab. 4. The calculation of the shape coefficient FC and specific energy SE for two drill bits, 16/25 and 25/40.

Rock sample (drill bit)	FF_1 (mm)	N_1 (%)	N_0 (%)	FF_0 (mm)	FC	SE (MJm^{-3})
L_3(16/25)	0.580	19.6	80.4	0.853	2.79	1,132.00
L_3(25/40)	0.627	19.8	80.2	0.813	3.13	1,067.71
L_4(16/25)	0.580	18.6	81.4	0.853	2.97	1,238.47
L_4(25/40)	0.580	17.5	82.5	0.810	3.37	1,326.97
G_1(16/25)	0.410	4.6	95.4	0.687	12.43	1,597.55
G_1(25/40)	0.420	12.1	87.9	0.767	3.98	3,200.61
L_7(16/25)	0.560	21.4	78.6	0.520	3.96	3,519.36
L_6(25/40)	0.577	24.0	76.0	0.507	3.60	4,355.58
G_2(16/25)	0.420	9.0	91.0	0.853	4.96	4,357.04
G_2(25/40)	0.580	19.7	80.3	0.833	2.84	4,045.38
L_8(16/25)	0.420	6.4	93.6	0.520	11.83	5,018.52
L_7(25/40)	0.590	20.9	79.1	0.507	4.40	4,594.49
G_3(16/25)	0.420	7.2	92.8	0.520	10.45	5,746.81
G_3(25/40)	0.580	13.1	86.9	0.500	7.69	2,595.84
L_9(16/25)	0.580	19.2	80.8	0.520	4.69	5,188.85
L_8(25/40)	0.645	21.9	78.1	0.840	2.73	3,780.95

Tab. 5. The calculation of the shape coefficient FC and specific energy SE for two drill bits of the same size diamonds, 16/25.

Rock sample	FF_1 (mm)	N_1 (%)	N_0 (%)	FF_0 (mm)	FC	SE (MJm^{-3})
L_{11}	0.543	23.3	76.7	0.833	2,15	1,200.60
L_{12}	0.590	22.5	77.5	0.847	2,40	1,210.72
L_{13}	0.580	19.8	80.2	0.840	2,80	1,176.54
A_1	0.21	5	95	0.83	4,62	2,014.73
A_2	0.59	17	83	0.49	5,97	1,656.60
A_3	0.54	17	83	0.77	3,42	1,884.28
L_{14}	0.604	27.2	72.8	0.792	2,04	1,558.29
L_{15}	0.590	21.9	78.1	0.820	2,57	1,104.44
L_{16}	0.600	22.5	77.5	0.847	2,44	1,110.50
A_4	0.41	12	88	0.49	6,35	2,121.48
A_5	0.60	27	73	0.50	3,21	1,946.08
A_6	0.61	28	72	0.51	3,14	2,037.40

3. Results

Figure 4 shows the relationship between the shape coefficient and penetration depth for two drill bits with diamond sizes of 16/25 and 25/40. As the penetration depth increased or decreased, the shape coefficient FC changed, leading to a percentage increase in elongated particles N_1 at the start of drilling. The larger particle size N_1, achieved using the 25/40 drill bit, increased the shape coefficient FC after drilling limestone samples L3(25/40) and L4(25/40). Using the 25/40 drill bit, we achieved a larger particle size N_1, which reduced the shape coefficient FC in the drilled granodiorite samples G1(25/40) – G3(25/40). Conversely, a smaller particle size N_1 caused an increase in the shape coefficient FC when using the 16/25 drill bit. Refer to Tab. 4. Of course, the significant increase in the FC coefficient after drilling samples of granodiorite was accompanied by a percentage decrease in the elongated particles N_1 when using a 16/25 drill bit, see Fig.2.

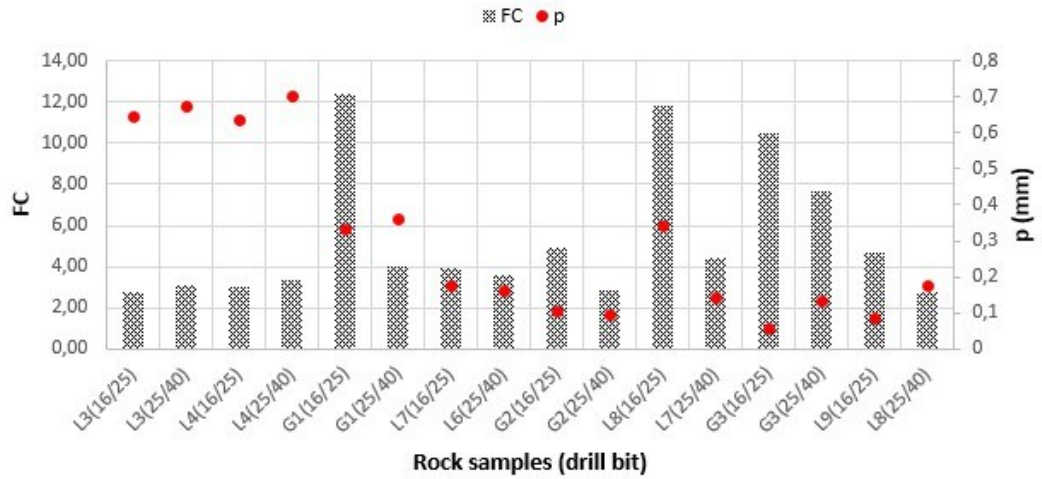

Fig. 4. Relationship between shape coefficient FC and penetration depth p (mm) of drilling into limestone and granodiorite using drill bits: 16/25 and 25/40.

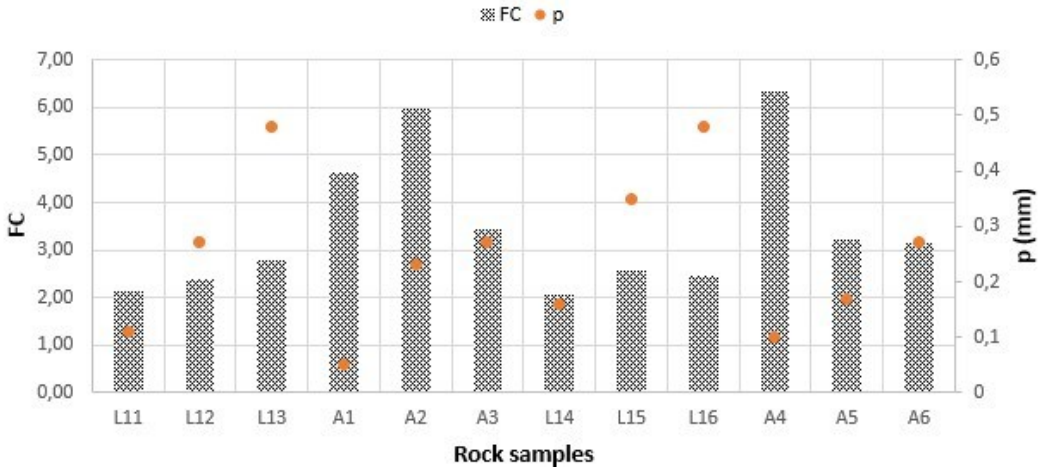

Fig. 5. Relationship between shape coefficient FC and penetration depth p (mm) of drilling into limestone and andesite using drill bits 16/25.

Granodiorite has the highest abrasiveness value of 1.4092 (mg·m⁻¹). Andesite's abrasiveness is 0.7913 mg·m⁻¹, while limestone's is 0.0186 mg·m⁻¹. We observed that greater abrasiveness results in greater changes in wear rate for larger diamonds (drill bit 16/25), thereby reducing the penetration depth of diamond core bits into the rock and decreasing the size of elongated particles, Fig.5 and Fig. 6. To capture changes in distribution shapes, we selected the similarly applied regimes (thrust force F and rotation speed of drill bit n), see Table 4 and Table 5, for rock samples L11, A2, G1.

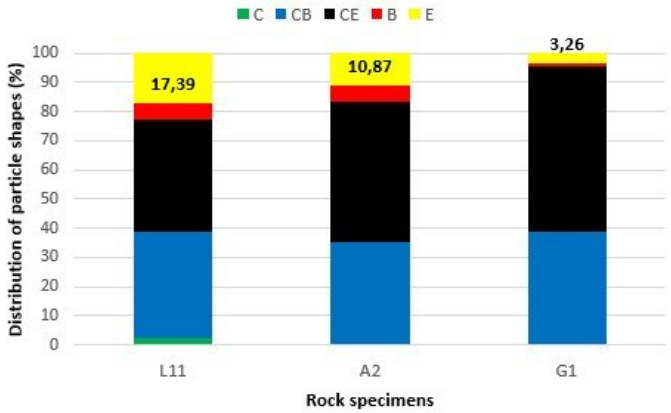

Fig. 6. Distribution of particle shapes of the analyzed class W2 with fractions (1mm – 0,4 mm) of drilling into limestone, andesite, and granodiorite using drill bit: 16/25.

Granodiorite, the most abrasive rock, resulted in the lowest penetration depth during drilling, and higher diamond wear was recorded on the 16/25 drill bit, increasing the shape coefficient FC due to a decrease in elongated particle shape. This is shown in Fig. 7a and Fig.7b.

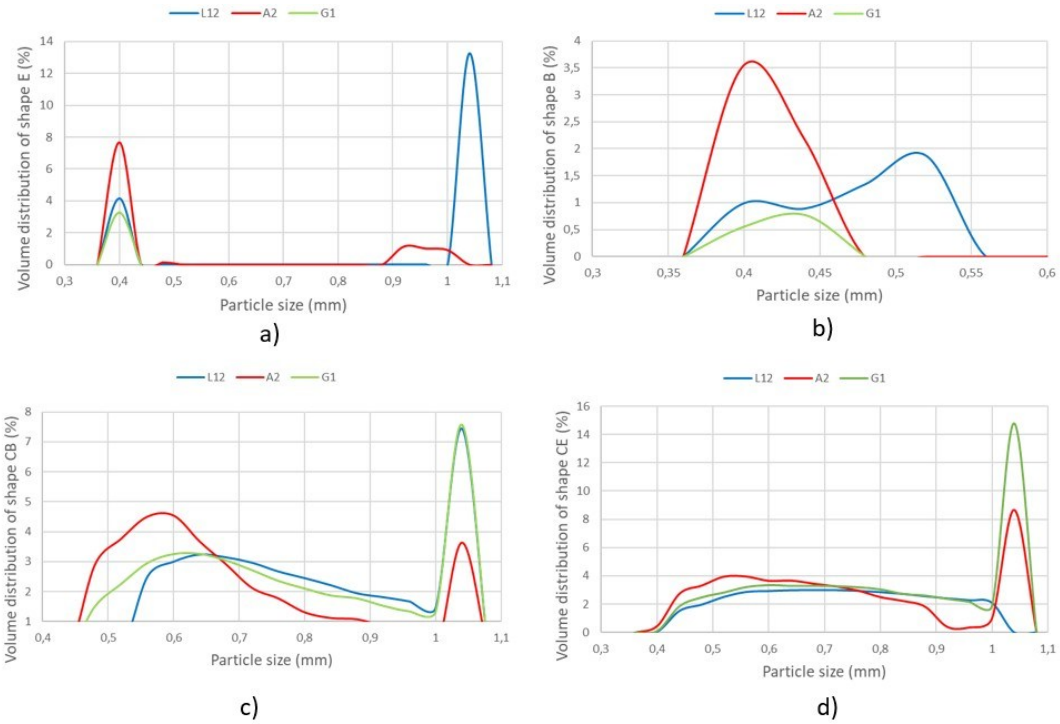

Fig. 7. Volume distribution of particle shapes of drilling into limestone, andesite, and granodiorite using drill bit: 16/25: a) E-elongate; b) B-bladed; c) CB- compact bladed; d) CE- compact elongate.

4. Conclusion

Quantitative analysis of rock particle geometry, which led to the calculation of the shape coefficient FC, involved two main steps: measuring grain shape and size, and calculating the percentage of elongated grains. However, FC alone does not capture all the rock's mechanical properties, as factors such as hardness and uniaxial compressive strength are not reflected in the shape coefficient but in the shapes of rock debris. Nevertheless, abrasiveness was indicated by the shape coefficient. As abrasiveness increases, the FC coefficient tends to rise for drilled rock types. Nevertheless, the characterization of rock debris shape could be a useful indicator for predicting rock type, mechanical properties, drillability, and wear characteristics.

Acknowledgments

This research was supported by projects VEGA 2/0090/23 and APVV-23-0364.

References

1. A. Ersoy and M.D. Waller, “Textural characterisation of rocks”, Engineering Geology 39, 123-136 (1995).
2. M. Bali Hudáková, A. Kiovský, V. Krúpa, P. Vavrek, E. Lazarová, L. Ivanicova, “The Evaluation of the Wear of Surface-set Diamond Drill Bits by Analysing the Rock Debris and Process Parameters”, Inżynieria Mineralna 30 (2), 1-7 (2025).
3. M. Ali Maroof, A. Mahboubi, A. Noorzad, Y. Safi, “A new approach to particle shape classification of granular materials”, Transportation Geotechnics 22, (2020), https://doi.org/10.1016/j.trgeo.2019.100296
4. Y. Ghasemi, M. Rajczakowska, A. Cwirzen, “Estimation of specific surface area of particles based on size distribution curve”, Magazine of Concrete Research 70 (10), 533–540 (2018).
5. J.C. Santamarina, K.A. Klein, Y.H. Wang, E. Prencke, “Specific Surface Determination and Relevance”, Canadian Geotechnical Journal, 39, 233-241(2002).
6. R.P. Chapuis, “Predicting the saturated hydraulic conductivity of soils: a review”, Bulletin of Engineering Geology and the Environment 71, 401–434 (2012).
7. G. Lees, “A new Method for Determining the Angularity of Particles”, Sedimentology 3, 2–21(1964).
8. E. D. Sneed and R. L. Folk, Pebbles in the lower Colorado river, Texas: A study in particle morphogenesis. The Journal of Geology, 66 (2), 114–150 (1958).
9. D. J. Graham and N. G. Midgley. “Graphical representation of particle shape using triangular diagrams: An Excel spreadsheet method”, Earth Surface Processes and Landforms 25(13), 1473–1477 (2000).
10. Google. (n.d.). Particle Shape Analysis. Available from https://serc.carleton.edu/files/NAGTWorkshops/sedimentary/activities/particle_shape.pdf